



# CHEMISTRY

## A European Journal



### Accepted Article

**Title:** Highly Porous Metalloporphyrin Covalent Ionic Frameworks with Well Defined Cooperative Functional Groups as Excellent Catalysts for CO<sub>2</sub> Cycloaddition

**Authors:** Jiahui Liu, Guoying Zhao, Ocean Cheung, Lina Jia, Zhenyu Sun, and Suojiang Zhang

This manuscript has been accepted after peer review and appears as an Accepted Article online prior to editing, proofing, and formal publication of the final Version of Record (VoR). This work is currently citable by using the Digital Object Identifier (DOI) given below. The VoR will be published online in Early View as soon as possible and may be different to this Accepted Article as a result of editing. Readers should obtain the VoR from the journal website shown below when it is published to ensure accuracy of information. The authors are responsible for the content of this Accepted Article.

**To be cited as:** *Chem. Eur. J.* 10.1002/chem.201900992

**Link to VoR:** <http://dx.doi.org/10.1002/chem.201900992>

Supported by  
**ACES**

WILEY-VCH

## FULL PAPER

# Highly Porous Metalloporphyrin Covalent Ionic Frameworks with Well Defined Cooperative Functional Groups as Excellent Catalysts for CO<sub>2</sub> Cycloaddition

Jiahui Liu,<sup>[a,b]</sup> Guoying Zhao,<sup>[b]</sup> Ocean Cheung,<sup>[c]</sup> Lina Jia,<sup>[b]</sup> Zhenyu Sun\*<sup>[a]</sup> and Suojiang Zhang\*<sup>[b]</sup>

**Abstract:** The development of multifunctional heterogeneous catalysts with high porosity and remarkable catalytic activity still remains the challenge. Herein, four highly porous metalloporphyrin covalent ionic frameworks (CIFs) were synthesized by coupling 5,10,15,20-tetrakis(4-nitrophenyl)porphyrin (TNPP) with 3,8-diamino-6-phenylphenanthridine (NPPN) or 5,5'-diamino-2,2'-bipyridine (NBPY) following ionized by using bromoethane (C<sub>2</sub>H<sub>5</sub>Br) or dibromoethane (C<sub>2</sub>H<sub>4</sub>Br<sub>2</sub>) and then metalize by Zn or Co. The resulting CIFs showed high efficiency in catalyzing the CO<sub>2</sub> cycloaddition of propylene oxide (PO) to form propylene carbonate (PC). All of the Zn containing CIF catalysts were able to catalyze the cycloaddition reaction with a PC yield of over 97%. The TNPP/NBPY (CIF2) catalyst ionized with C<sub>2</sub>H<sub>4</sub>Br<sub>2</sub> and metalized with Zn (Zn-CIF2-C<sub>2</sub>H<sub>4</sub>) exhibited the highest catalytic activity among the synthesized catalysts. The high catalytic performance of Zn-CIF2-C<sub>2</sub>H<sub>4</sub> was related to its large porosity (577 m<sup>2</sup>/g), high Br:metal ratio (1:3.89) as well as the excellent synergistic action between the Lewis acid Zn sites and the nucleophilic Br<sup>-</sup> ion. We found that Zn-CIF2-C<sub>2</sub>H<sub>4</sub> was stable that over 94% PC yield could be obtained even after 6 cycles. In addition, Zn-CIF2-C<sub>2</sub>H<sub>4</sub> could catalyze the CO<sub>2</sub> cycloaddition of several other epoxides. We are confident that these highly porous materials are promising multifunctional and efficient catalysts for industrial relevant reactions.

## Introduction

The development of new and efficient catalysts is a key part of implementing clean and sustainable chemical processes.<sup>[1]</sup> Generally, homogeneous catalysts show high catalytic activity because of their highly accessible and well-defined active sites. Natural enzyme catalysts typically combine multiple functional groups that can cooperate with each other into a confined space.<sup>[2]</sup> This gives enzyme catalysts enhanced catalytic activity, high selectivity of substrates, reactions and stereo structures.

Nevertheless, heterogeneous catalysts are often placed at the forefront of the chemical industry because they have several advantages over homogeneous, and natural enzyme catalysts. They have high stability and can stand relatively harsh reaction conditions. Unlike homogeneous catalysts, heterogeneous catalysts can easily be separated and recycled after a reaction. However, the active sites of heterogeneous catalysts are typically less available when compared with homogeneous catalysts, as a catalyzed reaction can only take place at the liquid/gas - solid interface (i.e. in the case of a solid catalyst in a liquid/gas phase reaction). As the active sites of heterogeneous catalysts are spatially fixed and separated in the rigid framework, the cooperative active sites found in homogeneous or enzyme catalysts are not usually found in heterogeneous catalysts.<sup>[3]</sup> It would be highly desirable to develop heterogeneous catalysts with some of the advantageous properties of homogeneous or enzyme catalysts, such as the highly accessible, well-defined and well-placed cooperative active sites. Such "biomimetic catalysts" would combine the advantages of homogeneous, enzyme and heterogeneous catalysts. Confining functional molecules into the pores of heterogeneous catalysts by physical impregnation is a possible approach to create a "hybrid catalyst", although leaching of the functional molecules is often a problem.<sup>[4]</sup> Integrating ionic modules into the framework of a heterogeneous catalyst could result in a framework containing free mobile functional counter ions with coulomb interactions.<sup>[5]</sup> This can promote a cooperative environmental for the different functional active sites within the framework. Furthermore, increasing the specific surface area and the active sites density of the multifunctional heterogeneous catalysts is an important aspect for improving the accessibility of the active sites. Both of these factors would further increase the catalytic activity of heterogeneous catalysts. Highly porous charged (cationic or anionic) polymers can be suitable multifunctional biomimetic catalysts, but their synthesis is difficult due to the strong coulomb interactions between building blocks that often resulted in the collapse of the pore structure.<sup>[6]</sup> Recently, covalent organic frameworks (COFs) with periodic rigid organic scaffold have gain significant attention in catalysis, gas separation and storage due to their high porosity, their chemical flexibility, structural diversity and stability.<sup>[7]</sup> Ionic liquids are a class of popular soft materials that have been tested and adopted in various applications. Ionic liquids are interesting due to their distinct ionic properties, including the ability to design specific ions, ion diversity, and ion synergy.<sup>[8]</sup> The incorporation of modular ionic liquids into the rigid organic scaffold of COF can stabilize the pores within these charged polymers. The functionality of ionic liquids can further broaden the application areas of COFs. Ionic liquids incorporated COFs can be an auspicious approach to develop novel efficient and stable biomimetic multifunctional catalysts.<sup>[9]</sup> The biomimetic catalysts would have periodic network

[a] J. Liu, Prof. Dr. Z. Sun  
State Key Laboratory of Organic-Inorganic Composites  
Beijing University of Chemical Technology  
Beijing, 1000029 (RP China)  
E-mail: sunzy@mail.buct.edu.cn

[b] J. Liu, Prof. Dr. G. Zhao, L. Jia, Prof. Dr. S. Zhang  
Institute of Process Engineering, Chinese Academy of Sciences  
Beijing, 100190 (RP China)  
E-mail: sjzhang@ipe.ac.cn

[c] Dr. O. Cheung  
Nanotechnology and Functional Materials Division, Department of  
Engineering Sciences  
The Ångström Laboratory, Uppsala University  
Box 534, SE-751 21 Uppsala, Sweden  
Supporting information for this article is given via a link at the end of  
the document.

## FULL PAPER

of catalytic active centers which are composed of multiple well-defined and well-placed cooperative active sites. CO<sub>2</sub> cycloaddition on epoxides to produce cyclic carbonate is a well-known chemical process in which heterogeneous catalysts play an important role. The process is also an effective and economical way of CO<sub>2</sub> utilization.<sup>[10]</sup> Cyclic carbonates produced from CO<sub>2</sub> cycloaddition can be used in various applications, including as excellent aprotic polar solvents, electrolytes in batteries, raw materials for the production of polycarbonates, polyurethane and some pharmaceuticals etc.<sup>[11]</sup> In order to achieve high reaction rate, it is essential that the nucleophilic halide anions and the Lewis acid sites are in close proximity to function cooperatively.<sup>[6a, 12]</sup> Various catalysts have been developed for CO<sub>2</sub> cycloaddition, including organic catalysts (N-heterocyclic carbene, ionic liquids, poly-ionic liquids etc), metal complexes (e.g. metal halides, metallsalen and metalloporphyrins, etc) and metal oxides.<sup>[13]</sup> Among these catalysts, metalloporphyrins (Por) and their derivatives, such as metalloporphyrin-based metal-organic frameworks [M(Por)MOF], metalloporphyrin-based organic polymers [M(Por)OP], metalloporphyrin immobilized on porous materials (zeolites, MOF or carbon nanotubes) have shown outstanding catalytic activities towards CO<sub>2</sub> cycloaddition.<sup>[6a, 14]</sup> However, in most of these cases, nucleophilic organic salts, such as tetrabutylammonium bromide (TBAB), are required. The addition of salts makes this catalytic process not truly heterogeneous. Bifunctional cationic porous organic polymer incorporated with both metalloporphyrin sites and nucleophilic sites were developed recently by Ji et al.<sup>[15]</sup> This catalyst also exhibited good catalytic activity and recyclability in CO<sub>2</sub> cycloaddition at atmospheric pressure without the use of any co-catalysts. On the other hand, the low Brunauer–Emmett–Teller (BET) surface area of these charged polymers is usually quite low, which limits the accessibility of the active sites and reduces their catalytic activity.

In this work, we illustrated the concept of designing biomimetic multifunctional heterogeneous catalyst that would be suitable for CO<sub>2</sub> cycloaddition on epoxides. Four nitro containing porphyrin (5,10,15,20-tetrakis(4-nitrophenyl)porphyrin (TNPP)) and two diamino compounds (3,8-diamino-6-phenylphenanthridine (NPPN) or 5,5'-diamino-2,2'-bipyridine (NBPY)) were chosen as rigid building blocks to synthesize a series of porous covalent ionic framework (CIF) via a sequential coupling between the nitro and amino groups. The synthesized CIFs were ionized post-synthesis (by quaternization) and subsequently metallized. A schematic of the processes behind the production of these novel multifunctional CIF catalysts can be found in Figure 1. Various characterization techniques were employed to characterize the synthesized catalysts, including Fourier transform infrared spectroscopy (FT-IR), Solid-state <sup>13</sup>C NMR spectroscopy, Energy dispersive X-ray spectroscopy (EDX), X-ray photoelectron spectroscopy (XPS), Thermogravimetric analysis (TGA), Inductively coupled plasma atomic emission spectroscopy (ICP-AES), Ion chromatography analysis (IC) and Nitrogen sorption. These multifunctional CIFs catalysts have high porosity and contain metalloporphyrin Lewis acid centers and bromide anions as nucleophile. The stoichiometry between metalloporphyrin and bromide ions was varied and the BET surface area was adjusted

by tailoring ionic liquid moieties. Furthermore, their catalytic performance in CO<sub>2</sub> cycloaddition on epoxides was systematically examined.

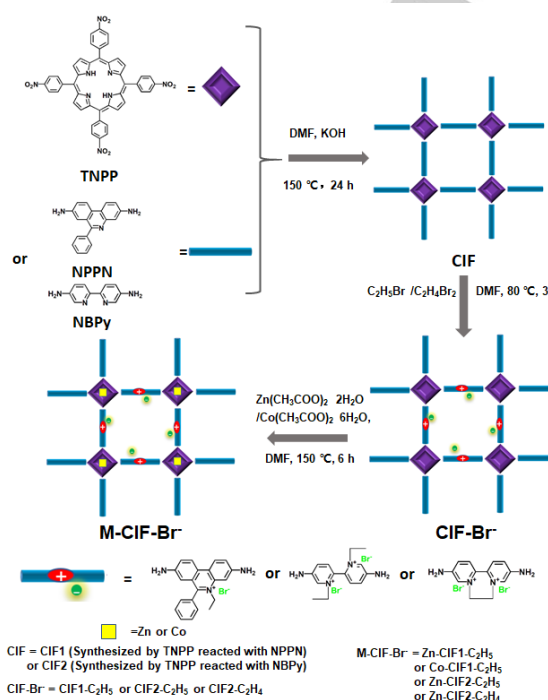


**Figure 1.** Schematic representation of the synthetic process of the metalloporphyrin-based covalent ionic frameworks (CIFs).

## Results and Discussion

### Preparation of catalysts

The multifunctional CIF catalysts (Figure 1) were prepared using a three step processes that involved 1) synthesis of CIF, 2) ionization by quaternization and 3) metallization. Two different types of CIF catalysts were synthesized. CIFs that were synthesized by coupling TNPP with NPPN were referred to as CIF1 in this study. Post-synthesis ionization on CIF1 was carried out using bromoethane (C<sub>2</sub>H<sub>5</sub>Br). The ionized CIFs (CIF1-C<sub>2</sub>H<sub>5</sub>) were then metallized with Zn or Co. This gave two CIF1 catalysts referred to as Zn-CIF1-C<sub>2</sub>H<sub>5</sub> and Co-CIF1-C<sub>2</sub>H<sub>5</sub>. We also synthesized another type of CIFs by coupling TNPP with NBPY (referred to as CIF2). Post-synthesis ionization of CIF2 was carried out using bromoethane (C<sub>2</sub>H<sub>5</sub>Br) or ethylene dibromide (C<sub>2</sub>H<sub>4</sub>Br<sub>2</sub>) to give CIF2-C<sub>2</sub>H<sub>5</sub> and CIF2-C<sub>2</sub>H<sub>4</sub>. CIF2-C<sub>2</sub>H<sub>5</sub> and CIF2-C<sub>2</sub>H<sub>4</sub> were metallized using Zn to give Zn-CIF2-C<sub>2</sub>H<sub>5</sub> and Zn-CIF2-C<sub>2</sub>H<sub>4</sub>. The four successfully synthesized multifunctional CIF catalysts were characterized using various methods as discussed below.

### Catalyst characterization

The X-Ray diffractograms (XRD) of Zn-CIF1-C<sub>2</sub>H<sub>5</sub>, Co-CIF1-C<sub>2</sub>H<sub>5</sub>, Zn-CIF2-C<sub>2</sub>H<sub>5</sub> and Zn-CIF2-C<sub>2</sub>H<sub>4</sub> (Figure S1) confirmed that these azo polymers were amorphous as expected for CIFs. The

## FULL PAPER

Scanning electron microscopy (SEM) images shown in Figure S2 suggested that these CIF catalysts were composed of agglomerated irregularly shaped particles. No distinctive particle size or shapes could be observed in any of the CIF catalysts. Thermogravimetric analysis (TGA) curve displayed in Figure 2 revealed that the Thermal degradation temperature ( $T_d=10\%$  weight loss under  $N_2$  atmosphere) of Zn-CIF1-C<sub>2</sub>H<sub>5</sub>, Zn-CIF2-C<sub>2</sub>H<sub>5</sub>, Zn-CIF2-C<sub>2</sub>H<sub>4</sub> and Co-CIF1-C<sub>2</sub>H<sub>5</sub> varied between 380 and 485°C. The TGA data demonstrated that these CIF catalysts were thermally stable because of the rigid structure of the azo polymer.<sup>[16]</sup> The porous polymer precursors CIF1 and CIF2, and the ionized CIF1-C<sub>2</sub>H<sub>5</sub>, CIF2-C<sub>2</sub>H<sub>5</sub>, CIF2-C<sub>2</sub>H<sub>4</sub> also exhibited excellent thermal stability (TGA curves shown in Figure S3).

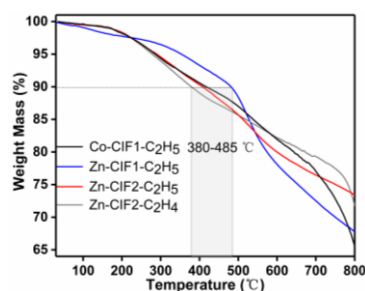


**Figure 2.** Thermogravimetric analysis (TGA) of metalloporphyrin CIFs (Co-CIF1-C<sub>2</sub>H<sub>5</sub>, Zn-CIF1-C<sub>2</sub>H<sub>5</sub>, Zn-CIF2-C<sub>2</sub>H<sub>5</sub>, and Zn-CIF2-C<sub>2</sub>H<sub>4</sub>) under  $N_2$  atmosphere up to 800°C at a heating rate 10°C min<sup>-1</sup>.

The IR spectra of the CIF catalysts can be found in Figure 3. The IR spectra of CIF1, CIF1-C<sub>2</sub>H<sub>5</sub>, Zn-CIF1-C<sub>2</sub>H<sub>5</sub> and Co-CIF1-C<sub>2</sub>H<sub>5</sub> in Figure 3a all contained an IR band centered at around 1597 cm<sup>-1</sup>, this band was related to the N=N group.<sup>[16]</sup> The presence of this N=N vibration band confirmed the successful coupling of the amino/nitro groups to form an “azo-bridge”. Additional IR bands at around 1520 cm<sup>-1</sup> and 1340 cm<sup>-1</sup> were also detected, these bands were related to the N=O stretching vibration and indicated the presence of unreacted terminal nitro groups from TNPP.<sup>[17]</sup> Two new bands at around 1452 and 1261 cm<sup>-1</sup> appeared after the successful ionization of phenanthridine. These bands were related to the methyl group after ionization. The IR band at around 997 cm<sup>-1</sup> was related to the in-plane metalloporphyrin deformation mode and only appeared in the metalized Zn-CIF1-C<sub>2</sub>H<sub>5</sub> and Co-CIF1-C<sub>2</sub>H<sub>5</sub>.<sup>[18]</sup> These bands confirmed the successful metalation of CIF1-C<sub>2</sub>H<sub>5</sub>.

The N=N (~1600 cm<sup>-1</sup>) and the N=O stretching (1520 and 1340 cm<sup>-1</sup>) bands were also observed in the IR spectra of CIF2, CIF2-C<sub>2</sub>H<sub>5</sub> and Zn-CIF2-C<sub>2</sub>H<sub>5</sub> shown in Figure 3b, as well as in the IR spectra of CIF2, CIF2-C<sub>2</sub>H<sub>4</sub> and Zn-CIF2-C<sub>2</sub>H<sub>4</sub> shown in Figure 3c. The in-plane metalloporphyrin deformation mode band at around 997 cm<sup>-1</sup> was also observed in the IR spectra of Zn-CIF2-C<sub>2</sub>H<sub>5</sub> and Zn-CIF2-C<sub>2</sub>H<sub>4</sub>. The bands that were related to the presence of the methyl (or methylene) group after ionization (at around 1452 and 1261 cm<sup>-1</sup>) also appeared on CIF2-C<sub>2</sub>H<sub>5</sub> (Figure 3b middle), Zn-CIF2-C<sub>2</sub>H<sub>5</sub> (Figure 3b bottom), CIF2-C<sub>2</sub>H<sub>4</sub> (Figure 3c middle), and Zn-CIF2-C<sub>2</sub>H<sub>4</sub> (Figure 3c bottom).

The solid state <sup>13</sup>C NMR spectra of the non-metalized CIFs are displayed in Figure 3d. The peak centered at around 150.9 ppm

was observed on all samples. This peak confirmed the formation of azo-linked aromatic carbon atoms as previously reported in literature.<sup>[17]</sup> The peaks related to methyl and methylene groups were also observed for CIF1-C<sub>2</sub>H<sub>5</sub>, CIF2-C<sub>2</sub>H<sub>5</sub> and CIF2-C<sub>2</sub>H<sub>4</sub> at 11, 45.4 and 49 ppm.<sup>[19]</sup>

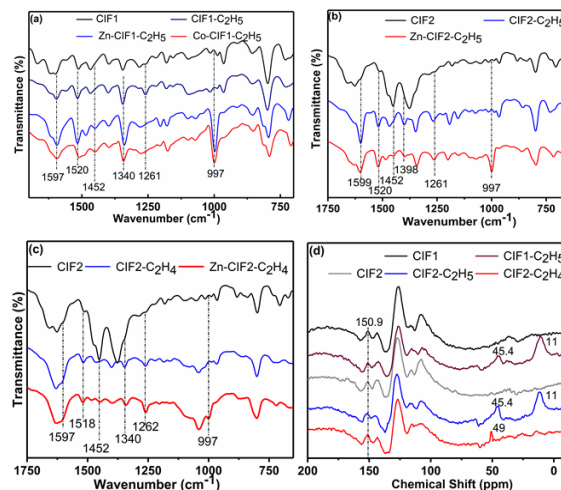


**Figure 3.** FT-IR spectra of a) CIF1, CIF1-C<sub>2</sub>H<sub>5</sub>, Zn-CIF1-C<sub>2</sub>H<sub>5</sub> and Co-CIF1-C<sub>2</sub>H<sub>5</sub>; b) CIF2, CIF2-C<sub>2</sub>H<sub>5</sub> and Zn-CIF2-C<sub>2</sub>H<sub>5</sub>; c) CIF2, CIF2-C<sub>2</sub>H<sub>4</sub> and Zn-CIF2-C<sub>2</sub>H<sub>4</sub>. d) Solid-state <sup>13</sup>C NMR spectra of CIF1, CIF1-C<sub>2</sub>H<sub>5</sub>, CIF2, CIF2-C<sub>2</sub>H<sub>5</sub> and CIF2-C<sub>2</sub>H<sub>4</sub>.

The N 1s XPS spectrum of CIF1, Co-CIF1-C<sub>2</sub>H<sub>5</sub>, and Zn-CIF1-C<sub>2</sub>H<sub>5</sub> is shown in the Supporting Information Figure S3. Three peaks were observed at around 401.0, 399.9 and 398.0 eV. These peaks corresponded to the pyrrolic nitrogen (-NH-), azo nitrogen (-N=N-) and imine nitrogen (-C=N-) of porphyrin ring and NPPN, respectively.<sup>[20]</sup> The N 1s XPS spectrum of CIF2 is shown in Figure 4a (top). Four peaks at 404.0, 400.7, 399.8, 398.0 eV were observed. These peaks corresponded to nitro nitrogen (Ph-NO<sub>2</sub>), pyrrolic nitrogen (-NH-), azo nitrogen (-N=N-) and imine nitrogen (-C=N-) of porphyrin ring and NBPY, respectively. The N 1s XPS spectrum of Zn-CIF2-C<sub>2</sub>H<sub>5</sub> and Zn-CIF2-C<sub>2</sub>H<sub>4</sub> (Figure 4a, middle and bottom) both showed one new peak at 401.8 eV, indicating the appearance of ionic pyridine near the surfaces.<sup>[6b]</sup> The Br 3d XPS spectra of Zn-CIF1-C<sub>2</sub>H<sub>5</sub> in Figure 4b (top) showed three peaks at 70.3, 68.25 and 67.04 eV. The Br 3d XPS spectrum (Figure S3b) for Co-CIF1-C<sub>2</sub>H<sub>5</sub> displayed two weak peaks at 70.3 and 68.5 eV. Only two peaks were observed in the Br 3d XPS spectrum of Zn-CIF2-C<sub>2</sub>H<sub>5</sub> (at 68.83, 67.74 eV Figure 4b, middle) and Zn-CIF2-C<sub>2</sub>H<sub>4</sub> (at 69.13 and 68.06 eV Figure 4b, bottom). The small shift in their Br binding energy indicated that there is a similar level of interaction between the cationic frameworks of CIFs and Branions in Zn-CIF2-C<sub>2</sub>H<sub>5</sub> and Zn-CIF2-C<sub>2</sub>H<sub>4</sub>. The absence of any peaks between 71 to 73 eV indicated that there were no C-Br bonds present on these CIFs. The Zn 2p XPS spectra of Zn-CIF1-C<sub>2</sub>H<sub>5</sub>, Zn-CIF2-C<sub>2</sub>H<sub>5</sub> and Zn-CIF2-C<sub>2</sub>H<sub>4</sub> are shown in Figure 4c. In all three cases two peaks were observed, the Zn 2P 1/2 peak (at 1044.7 and 1046.7 eV) and the Zn 2P 3/2 peak (at 1021.6 and 1023.5 eV). These peaks confirmed the presence of Zn.<sup>[4b]</sup> In the case of Co-CIF1-C<sub>2</sub>H<sub>5</sub> (Figure S3c), four peaks were observed in the Co 2p XPS spectrum, which

## FULL PAPER

suggested that cobalt ions exist in a mixed valence state in Co-CIF1-C<sub>2</sub>H<sub>5</sub>.<sup>[21]</sup>

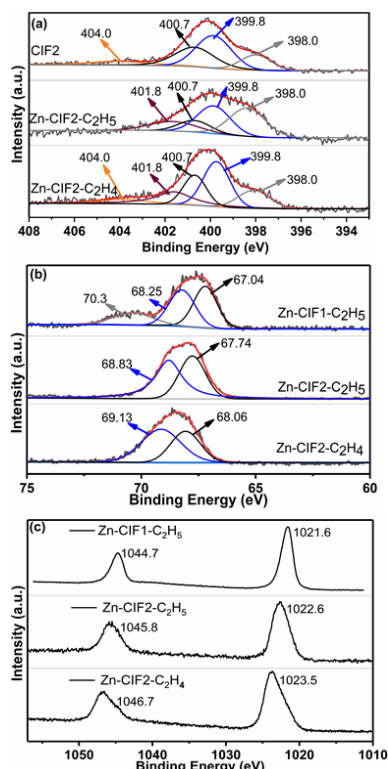


**Figure 4.** a) N 1s XPS spectra of CIF2, Zn-CIF1-C<sub>2</sub>H<sub>5</sub> and Zn-CIF2-C<sub>2</sub>H<sub>4</sub>. b) Br 3d XPS spectra of Zn-CIF1-C<sub>2</sub>H<sub>5</sub>, Zn-CIF2-C<sub>2</sub>H<sub>5</sub> and Zn-CIF2-C<sub>2</sub>H<sub>4</sub>. c) Zn 2p XPS spectra of Zn-CIF1-C<sub>2</sub>H<sub>5</sub>, Zn-CIF2-C<sub>2</sub>H<sub>5</sub> and Zn-CIF2-C<sub>2</sub>H<sub>4</sub>.

The metal and Br content of the CIF catalysts were analyzed using ICP-AES and IC analysis. Table 1 shows the elemental composition of these elements. The Zn content of the Zn-CIF1-C<sub>2</sub>H<sub>5</sub>, Zn-CIF2-C<sub>2</sub>H<sub>5</sub> and Zn-CIF2-C<sub>2</sub>H<sub>4</sub> catalysts were approximately 0.48, 0.45 and 0.40 mmol/g, respectively according to the ICP-AES. The Co-CIF1-C<sub>2</sub>H<sub>5</sub> catalyst had a Co content of 0.46 mmol/g. The Br content of Co-CIF1-C<sub>2</sub>H<sub>5</sub>, Zn-CIF1-C<sub>2</sub>H<sub>5</sub>, Zn-CIF2-C<sub>2</sub>H<sub>5</sub>, and Zn-CIF2-C<sub>2</sub>H<sub>4</sub> varied from 0.91 to 1.75 mmol/g based on IC results. Additionally, the molar ratios of Br:Zn or Br:Co were calculated based on the Br, Zn and Co content (Table 1). The Br:Co ratio was 1:1.98 on Co-CIF1-C<sub>2</sub>H<sub>5</sub>. The Br:Zn ratio was 1:1.90 on Zn-CIF1-C<sub>2</sub>H<sub>5</sub>, 1:3.89 on Zn-CIF2-C<sub>2</sub>H<sub>5</sub> and 1:3.95 on Zn-CIF2-C<sub>2</sub>H<sub>4</sub>.

The N<sub>2</sub> adsorption isotherm of all CIF catalysts are shown in Figure 5 and the BET specific surface area and pore volume are summarized in Table 1. All of the synthesized catalysts showed high porosity with BET surface area ranging from 281 to 815 m<sup>2</sup>/g. As expected, the metal-free, as-synthesized CIF-1 and CIF-2 had the highest BET surface area when compared with their respective ionized and metallized CIFs. It is important to note that the CIF catalysts showed high BET surface area even after ionization and metallization, which would allow the active catalyst sites to be more available when compared with low surface area solid catalysts. The specific BET surface area and total pore volume of the CIF catalysts after ionization and metallization decreased, which was expected due to the addition of the heavy

Br<sup>-</sup> and metal ions. Despite that, significant porosity was still detected for all CIF catalysts.

**Table 1** Physiochemical parameters of as-synthesized polymer CIF1, CIF2 and ionized and metallized CIFs Zn-CIF1-C<sub>2</sub>H<sub>5</sub>, Co-CIF1-C<sub>2</sub>H<sub>5</sub>, Zn-CIF2-C<sub>2</sub>H<sub>5</sub>, Zn-CIF2-C<sub>2</sub>H<sub>4</sub>.

| Sample                                | S <sub>BET</sub> <sup>[a]</sup> (m <sup>2</sup> /g) | V <sub>p</sub> <sup>[b]</sup> (cm <sup>3</sup> /g) | Br <sup>[c]</sup> (mmol/g) | Metal content <sup>[d]</sup> (mmol/g) | M:Br <sup>[e]</sup> |
|---------------------------------------|---|--|----------------------------|---------------------------------------|---------------------|
| CIF1                                  | 433.6   | 0.43   | -                          | -                                     | -                   |
| Zn-CIF1-C <sub>2</sub> H <sub>5</sub> | 289.0   | 0.36   | 0.91                       | 0.48 (Zn)                             | 1:1.90 (Zn:Br)      |
| Co-CIF1-C <sub>2</sub> H <sub>5</sub> | 281.4   | 0.36   | 0.91                       | 0.46 (Co)                             | 1:1.98 (Co:Br)      |
| CIF2                                  | 815.4   | 0.89   | -                          | -                                     | -                   |
| Zn-CIF2-C <sub>2</sub> H <sub>5</sub> | 465.4   | 0.40   | 1.75                       | 0.45 (Zn)                             | 1:3.89 (Zn:Br)      |
| Zn-CIF2-C <sub>2</sub> H <sub>4</sub> | 577.4   | 0.72   | 1.58                       | 0.40 (Zn)                             | 1:3.95 (Zn:Br)      |

[a] Surface area calculated based on the BET model from the nitrogen adsorption isotherm (P/P<sub>0</sub>=0.01–0.25). [b] The total pore volume calculated at P/P<sub>0</sub>=0.99. [c] The results of Br content were measured using ion chromatography (IC). [d] Calculated by ICP analysis. [e] The ratio of metal content to Br was calculated by the results of ICP and IC.

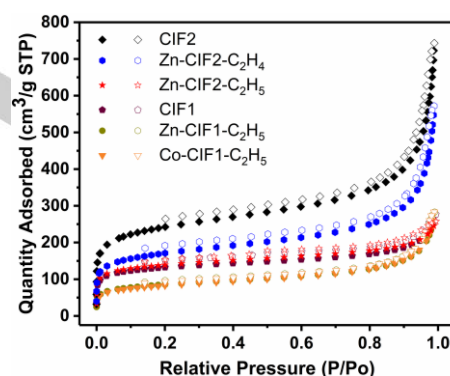


**Figure 5.** N<sub>2</sub> adsorption (filled) and desorption (empty) isotherm of CIF2, Zn-CIF2-C<sub>2</sub>H<sub>4</sub>, Zn-CIF2-C<sub>2</sub>H<sub>5</sub>, CIF1, Zn-CIF1-C<sub>2</sub>H<sub>5</sub> and Co-CIF1-C<sub>2</sub>H<sub>5</sub> at 77 K.

### Catalyst performance

The synthesized CIF catalysts were tested for their catalytic activities in CO<sub>2</sub> cycloaddition of propylene oxide (PO) to form propylene carbonate (PC). Table 2 gives a summary of the catalytic performance of the CIF catalysts included in this study. The synthesized CIFs (metallized and non-metallized) were tested together with Zn-TNPP as well as with a mixture containing Zn-TNPP/TBAB. By comparing Entry 1-4 (Table 2) it was clear that the Zn-CIF1-C<sub>2</sub>H<sub>5</sub> catalyst performed better than CIF-C<sub>2</sub>H<sub>5</sub>, Zn-TNPP and Zn-TNPP/TBAB. Zn-CIF1-C<sub>2</sub>H<sub>5</sub> was able to achieve 97% PC yield after 8 h, which was a much higher yield than Zn-TNPP (8%), Zn-TNPP/TBAB (77%) and CIF1-C<sub>2</sub>H<sub>5</sub> (37%). The high catalytic activity observed for Zn-CIF1-C<sub>2</sub>H<sub>5</sub> indicated the structure-specific synergy of Lewis acid Zn metal sites and nucleophile Br anions.<sup>[22]</sup> Furthermore, Zn-CIF1-C<sub>2</sub>H<sub>5</sub> had high BET surface area and porosity, allowing high accessibility to the

## FULL PAPER

catalytic sites. There was also a high amount of nucleophile Br anion in the vicinity of the Zn sites on Zn-CIF1-C<sub>2</sub>H<sub>5</sub>, which would enhance the catalytic activity as these sites could cooperate with one another.<sup>[23]</sup>

Catalysts performance were also carried out under harsh conditions (Entry 5-6, Table 2). Yield of 69% was obtained at 0.1 MPa for 8 h at 120 °C by catalysed by Zn-CIF1-C<sub>2</sub>H<sub>5</sub>. A longer reaction time at 0.1 MPa for 140 h at room temperature of Zn-CIF1-C<sub>2</sub>H<sub>5</sub> was also carried out and gave the 65% PC yield.

| Table 2. Catalytic performance of the cycloaddition reaction of CO <sub>2</sub> with PO over various catalysts. <sup>[a]</sup> |                                       |        |         |          |                          |                         |
|--|---------------------------------------|--------|---------|----------|--------------------------|-------------------------|
| Entry  | Catal.                                | T (°C) | P (Mpa) | time (h) | Yield <sup>[b]</sup> (%) | Sel. <sup>[c]</sup> (%) |
| 1  | Zn-TNPP                               | 120    | 2.5     | 8        | 8                        | >99                     |
| 2 <sup>[d]</sup>   | Zn-TNPP/TBAB                          | 120    | 2.5     | 8        | 77                       | >99                     |
| 3 <sup>[e]</sup>   | CIF1-C <sub>2</sub> H <sub>5</sub>    | 120    | 2.5     | 8        | 37                       | >99                     |
| 4  | Zn-CIF1-C <sub>2</sub> H <sub>5</sub> | 120    | 2.5     | 8        | 97                       | >99                     |
| 5  | Zn-CIF1-C <sub>2</sub> H <sub>5</sub> | 120    | 0.1     | 8        | 69                       | >99                     |
| 6  | Zn-CIF1-C <sub>2</sub> H <sub>5</sub> | 25     | 0.1     | 140      | 65                       | >99                     |
| 7  | Co-CIF1-C <sub>2</sub> H <sub>5</sub> | 120    | 2.5     | 8        | 82                       | >99                     |
| 8  | Zn-CIF2-C <sub>2</sub> H <sub>5</sub> | 120    | 2.5     | 5        | 98                       | >99                     |
| 9  | Zn-CIF2-C <sub>2</sub> H <sub>4</sub> | 120    | 2.5     | 4        | 97                       | >99                     |

[a] Reaction conditions: PO (3.0 mmol), catalyst (0.18 mol%). [b] Determined by using GC with ethyl acetate as an external standard. [c] The selectivity of PC. [d, e] The catalyst loading of TBAB and CIF1-C<sub>2</sub>H<sub>5</sub> was 0.34 mol% respected to the Br content.

The catalytic performance of Co-CIF1-C<sub>2</sub>H<sub>5</sub>, Zn-CIF2-C<sub>2</sub>H<sub>5</sub> and Zn-CIF2-C<sub>2</sub>H<sub>4</sub> could also be found in Table 2 (Entry 7-9). The same reaction conditions as Entry 1-4 were chosen for these experiments (120°C, 2.5 MPa, 0.18 mol% catalyst loading). Co-CIF1-C<sub>2</sub>H<sub>5</sub> showed the lowest PC yield of 82% after 8 h. The lower activity of Co-CIF1-C<sub>2</sub>H<sub>5</sub> was due to the lower Lewis acidity of Co (II) when compared with Zn (II) (Figure 4c and Figure S3c). Zn-CIF2-C<sub>2</sub>H<sub>5</sub> and Zn-CIF2-C<sub>2</sub>H<sub>4</sub> both reached the maximum PC yield level in less than 8 h. Zn-CIF2-C<sub>2</sub>H<sub>4</sub> required only 4 hours to reach a PC yield of 97%, which was one hour less than Zn-CIF2-C<sub>2</sub>H<sub>5</sub> (5 hours) and four hours less than Zn-CIF1-C<sub>2</sub>H<sub>5</sub> (8 hours). This is at least comparable to some recently reported functional polymers (Table S1). The reasons for the high catalytic activity of Zn-CIF2-C<sub>2</sub>H<sub>5</sub> and Zn-CIF2-C<sub>2</sub>H<sub>4</sub> could be related to the following separate factors: 1) their BET surface area and Br:metal ratio (Table 1) of Zn-CIF2-C<sub>2</sub>H<sub>5</sub> and Zn-CIF2-C<sub>2</sub>H<sub>4</sub> were both higher than Zn-CIF1-C<sub>2</sub>H<sub>5</sub>. Yang et al. have previously discussed the importance of the Br:metal ratio of a catalyst's ability to catalyze reactions.<sup>[6a, 12]</sup> Their findings would also explain the high catalytic activity of Zn-CIF2-C<sub>2</sub>H<sub>5</sub> and Zn-CIF2-C<sub>2</sub>H<sub>4</sub>. 2) The alkylbipyridine cation is less bulky than the alkylphenylphenanthridine cation, which may be beneficial for the cooperation between the Lewis acid Zn metal sites and nucleophile Br anions.

The kinetic curves of the CO<sub>2</sub> cycloaddition experiments for the four synthesized CIF catalysts (Entry 4, 7-9) can be found in Figure 6. Figure 6 shows that Zn-CIF2-C<sub>2</sub>H<sub>4</sub> had the fastest reaction kinetics out of the tested CIF catalysts. The reaction

kinetics of Zn-CIF2-C<sub>2</sub>H<sub>5</sub> was comparable with that of Zn-CIF2-C<sub>2</sub>H<sub>4</sub>, although the differences were clear. Zn-CIF2-C<sub>2</sub>H<sub>4</sub> showed faster reaction kinetics and reached full conversion more quickly. As the Br:metal ratios of Zn-CIF2-C<sub>2</sub>H<sub>4</sub> (1:3.95) and Zn-CIF2-C<sub>2</sub>H<sub>5</sub> (1:3.89) were similar (Table 1), the high BET surface area and pore volume of on Zn-CIF2-C<sub>2</sub>H<sub>4</sub> (577.4 m<sup>2</sup>/g, 0.72 cm<sup>3</sup>/g) may be responsible for the faster reaction kinetics. The relatively lower reaction kinetics observed for Zn-CIF1-C<sub>2</sub>H<sub>5</sub> and Co-CIF1-C<sub>2</sub>H<sub>5</sub> was mainly the result of both low BET surface area and low Br:metal ratios. Results from a hot filtration experiments of Zn-CIF2-C<sub>2</sub>H<sub>4</sub> is presented in the Figure 6. Zn-CIF2-C<sub>2</sub>H<sub>4</sub> was filtered after the reaction was carried out for 1 h, while the filtrate was heated under the same conditions for another 7 h. A slight increase in the PC yield was observed after 7 h compared with that measured at 1 h, confirming a small amount of leaching of the active phase of the solid catalysts.

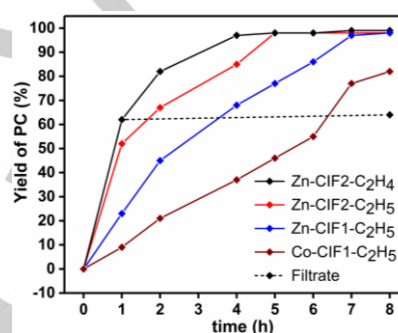


**Figure 6.** Kinetic curves for PO cycloaddition reactions using metalloporphyrin CIFs (Zn-CIF2-C<sub>2</sub>H<sub>4</sub>, Zn-CIF2-C<sub>2</sub>H<sub>5</sub>, Zn-CIF1-C<sub>2</sub>H<sub>5</sub>, and Co-CIF1-C<sub>2</sub>H<sub>5</sub>) as the catalysts. Reaction conditions: PO (3.0 mmol), catalyst (0.18 mol% based on metal content), initial CO<sub>2</sub> pressure 2.5 Mpa at 120°C. The filtrate test was performed by removing the Zn-CIF2-C<sub>2</sub>H<sub>4</sub> from the reaction system after 1 h.

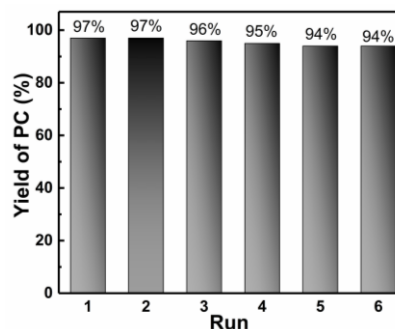


**Figure 7.** Catalyst reusability of Zn-CIF2-C<sub>2</sub>H<sub>4</sub>. Reaction conditions: PO (3.0 mmol), catalyst (0.18 mol% based on metal content), initial CO<sub>2</sub> pressure 2.5 Mpa, for 4 hours at 120°C.

The cycle stability of the best performing Zn-CIF2-C<sub>2</sub>H<sub>4</sub> catalyst was tested by performing the CO<sub>2</sub> cycloaddition experiment in cycles at 120°C for 4 h at 2.5 MPa (with PO). At the end of each cycle the CIF catalyst was recovered by centrifugation. The recovered CIF catalyst was washed and dried before being employed in the next cycle. The PC yields at of each cycle are depicted in Figure 7. There was no significant loss in the PC yield and selectivity (over 99% of the original) after 6 cycles. The SEM image and FTIR spectrum of the reused Zn-CIF2-C<sub>2</sub>H<sub>4</sub> were

## FULL PAPER

confirmed, and the morphology and structure of the catalyst showed no obvious change (Figure S5). Moreover, reused Zn-CIF2-C<sub>2</sub>H<sub>4</sub> has Zn content of 0.38 mmol/g, which is comparable to that of the fresh value (0.40 mmol/g). This clearly verifies that it is a stable catalyst candidate for this reaction.

We hereby propose a possible reaction mechanism for CO<sub>2</sub> cycloaddition of PO as illustrated in Figure 8. The (Zn or Co) metal sites are the Lewis acid sites which are located in the porphyrin part of the CIF structure. The nucleophilic sites are represented by Br<sup>-</sup> anions. At first, the oxygen on the epoxide comes in contact with the metal sites, activating the epoxide and an M-O bond is formed. Thereafter, the Br<sup>-</sup> nucleophile attacks the β-carbon atom of the epoxy group from the side with low steric hindrance, this leads to the formation of a Br anion alkoxide intermediate. Then, the addition of CO<sub>2</sub> produces an M-carbonate intermediate which further cleaves the cyclic carbonate via an intramolecular ring closure step. Simultaneously, the catalyst is regenerated.

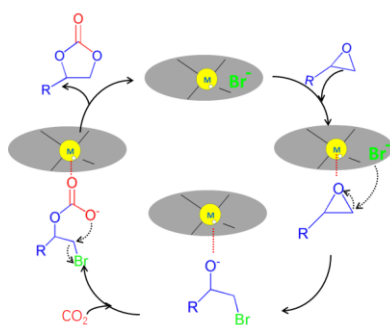


**Figure 8.** Representation of the catalytic mechanism for the cycloaddition of epoxide and CO<sub>2</sub> into cyclic carbonate catalyzed by these ionized and metalized CIFs

**Table 3.** Cycloaddition of CO<sub>2</sub> with various epoxides<sup>[a]</sup>.

| Substrate | Product | Zn-CIF2-C <sub>2</sub> H <sub>4</sub> |            | Zn-CIF1-C <sub>2</sub> H <sub>5</sub> |            |
|-----------|---------|---------------------------------------|------------|---------------------------------------|------------|
|           |         | Con. (%)                              | Selec. (%) | Con. (%)                              | Selec. (%) |
|           |         | 98                                    | >99        | 98                                    | >99        |
|           |         | 99                                    | >99        | 43                                    | 91         |
|           |         | 95                                    | >99        | 85                                    | >99        |
|           |         | 83                                    | >99        | 59                                    | 89         |

[a] Reaction conditions: substrate (3.0 mmol), catalyst (0.18 mol%), initial CO<sub>2</sub> pressure 2.5 MPa, 4 h for Zn-CIF2-C<sub>2</sub>H<sub>4</sub> (8 h for Zn-CIF1-C<sub>2</sub>H<sub>5</sub>).

To further investigate the catalytic ability of these ionized and metalized CIF catalysts for other epoxides, Zn-CIF1-C<sub>2</sub>H<sub>5</sub> and Zn-CIF2-C<sub>2</sub>H<sub>4</sub> were tested in CO<sub>2</sub> cycloaddition of four different epoxides. The chosen epoxides were epichlorohydrin (ECH), epoxy pentane (EP), styrene oxide (SO) and allyl glycidyl ether (AGE) and the same reaction conditions as for PO were used.

Table 3 shows that the CIF catalysts were able to catalyze the CO<sub>2</sub> cycloaddition reactions in all cases. Zn-CIF2-C<sub>2</sub>H<sub>4</sub> gave very high yield (over 95%) for ECH, EP and SO. The CO<sub>2</sub> cycloaddition of AGE gave the lowest yield (83%). The selectivity in all cases was close to 100%, which confirmed that Zn-CIF2-C<sub>2</sub>H<sub>4</sub> is a promising multifunctional catalyst for CO<sub>2</sub> cycloaddition of epoxides. Zn-CIF1-C<sub>2</sub>H<sub>5</sub> was also able to catalyze the CO<sub>2</sub> cycloaddition of all of the tested epoxides, but the yield for EP, SO and AGE was lower than Zn-CIF2-C<sub>2</sub>H<sub>4</sub> (note that the reactions using Zn-CIF1-C<sub>2</sub>H<sub>5</sub> ran for 8 h instead of 4 h). The comparatively low yield was probably related to the low BET surface area and the low Br:metal ratios on Zn-CIF1-C<sub>2</sub>H<sub>5</sub> when compared with Zn-CIF2-C<sub>2</sub>H<sub>4</sub> as discussed earlier.

## Conclusions

Two highly porous CIFs (CIF1 and CIF2) were synthesized by coupling TNPP with NPPN or NBPY. Post-synthesis ionization and metallization of these CIFs resulted in a selection of multifunctional CIF catalysts. For CO<sub>2</sub> cycloaddition of PO, all of the ionization and metallization CIF catalysts showed enhanced catalytic activity over Zn-TNPP and as-synthesized CIFs. The enhanced catalytic activity was due to the highly accessible reactive sites provided on the CIF highly porous materials. The well placed functional active sites also provided a synergistic catalytic environment between the Br<sup>-</sup> anion and the metal sites. The reaction temperature, pressure and catalyst loading all had an effect on the PC yield. Zn-CIF2-C<sub>2</sub>H<sub>4</sub> showed the highest catalytic activity of all of the catalysts synthesized with a PC yield of over 97% within 4 h (0.18 mol% catalyst, 120°C, 2.5 MPa). The high catalytic activity was the result of the high porosity and high Br:metal ratio of Zn-CIF2-C<sub>2</sub>H<sub>4</sub>. Cyclic experiment confirmed that Zn-CIF2-C<sub>2</sub>H<sub>4</sub> was stable, with over 95% of the original yield retained after 6 cycles. We demonstrated here that CIFs can be developed into efficient multifunctional heterogeneous catalyst for CO<sub>2</sub> cycloaddition of epoxides. The flexibility of the CIF structures and the numerous possibility for post-synthesis functionalization will no doubt put CIFs at the forefront of the development of functional materials.

## Experimental Section

### Materials

Materials Unless otherwise specified, all chemicals and reagents used in this study were of analytical grade and were used without further purification. N,N-Dimethylformamide (DMF), Potassium hydroxide (KOH), Zinc(II) acetate dihydrate, Cobalt(II) acetate tetrahydrate and anhydrous methanol were purchased from Xilong Chemical Co., Ltd., China. 4-Nitrobenzaldehyde and pyrrole were obtained from Aladdin Chemical Co., Ltd., China. Bromoethane (C<sub>2</sub>H<sub>5</sub>Br), dibromoethane (C<sub>2</sub>H<sub>5</sub>Br<sub>2</sub>), epichlorohydrin (ECH), epoxy pentane (EP), styrene oxide (SO) and allyl glycidyl ether (AGE) were purchased from Macklin Chemical Reagents Co., Ltd., China. De-ionized water (99.5%) was obtained from home built distillation assembly. 3,8-Diamino-

## FULL PAPER

6-phenylphenanthridine (NPPN) and 5,5'-diamino-2,2'-bipyridine (NBPY) were purchased from Zhengzhou Anmusi Chemical Products Co., Ltd.

**Instrumental characterization**

The N<sub>2</sub> adsorption-desorption isotherms were recorded using a Micromeritics ASAP 2020 HD surface area and porosity analyzer at 77 K. Before the sorption experiments, the samples were outgassed at 120°C for 4 hours. The BET surface area was calculated from the adsorption data at a relative pressure P/P<sub>0</sub> in the range of 0.01–0.25. The total pore volume was calculated at P/P<sub>0</sub> of 0.99. SEM experiments were carried out using a Hitachi SU8020 scanning electron microscope equipped with an EDS detector at an accelerating voltage of 5 kV for imaging, and 20 kV for EDS. FT-IR spectra were recorded using a Thermo Electron Corporation Nicolet 380 IR spectrometer in the range of 400–4000 cm<sup>-1</sup> (KBr pellets were prepared). TGA curves were recorded using a Shimadzu TA-60WS Thermal analyzer in the range of 30–800°C at a heating rate of 10°C min<sup>-1</sup> under nitrogen with flow rate of 30 ml/min. Solid state NMR spectra were obtained using a Bruker 500 MHz spectrometer equipped with a magic-angle spin probe. The Zn or Co content in the samples was determined by ICP-AES was carried out using a Shimadzu Plasma Atomic Emission Spectrometer. H<sub>2</sub>SO<sub>4</sub>/HNO<sub>3</sub> (1:1, V:V) was used as the solvent. Powder X-ray diffraction (PXRD) data were collected on a Bruker AXS D8 Advance A25 Powder X-ray diffractometer (40 kV, 40 mA) using CuKα (λ=1.5406 Å) radiation. Elemental analyzes were performed via flask combustion followed by ion chromatography using a ThermoFisher ICS-900 Dionex, with a 4.0×250 mm analytical column.

**Synthesis of Catalysts**

**Synthesis of TNPP:** 22.0 g 4-Nitrobenzaldehyde (1.45 × 10<sup>-1</sup> mol) and 24.0 mL of acetic anhydride (2.54 × 10<sup>-1</sup> mol) were dissolved in 600 mL of propionic acid in a 1 L round-bottom flask. The solution was then refluxed at 120°C for 30 min. After 30 min, 10.0 mL of pyrrole (1.44 × 10<sup>-1</sup> mol) was slowly added to the mixture. After refluxing for a further 30 min at 120°C, the reaction mixture was cooled to give a precipitate. This precipitate was collected by filtration, washed with H<sub>2</sub>O and methanol, and then dried under vacuum (80°C) and a powder was obtained. 1.5 g of the powder was then dissolved in pyridine (160 mL) in a 250 mL round-bottom flask and refluxed for 1 h at 80°C. The mixture was cooled after reflux and the solid content was collected by filtration and washed with acetone. 5,10,15,20-tetrakis(4-nitrophenyl)-21H,23H-porphine (TNPP) as a purple crystal with 14% yield was obtained thereafter. UV absorption at 432 nm (DMF), 516 nm (Soret), 550 nm, 591 nm and 646 nm (Q bands) was observed.

**Synthesis of CIF1 and CIF2:** 0.20 g of TNPP (0.3 mmol) and 0.171 g of NPPN (0.6 mmol) or 0.056 g of NBPY (0.6 mmol) was dissolved in 40 mL of DMF in a three-necked round-bottom flask equipped with a condenser, thermocouple and magnetic stirrer. 0.16 g of KOH (2.86 mmol) was added to this solution then stirring at room temperature for 10 min. The temperature of the reaction mixture was increased slowly up to 150°C with vigorous stirring under N<sub>2</sub> atmosphere. The reaction was left stirring 150°C for 24

h before cooling down to room temperature. 80 mL of distilled H<sub>2</sub>O was added to the reaction mixture and it was stirred for an additional 1 h. The resulting black precipitate was filtered and then washed 5 times individually with DMF, H<sub>2</sub>O and methanol in this order. Subsequently, precipitates were dried at 60°C under vacuum for 8 h to yield CIF1 or CIF2 with 57%, 66% yield, respectively.

All ionized CIF1 and CIF2 were prepared by quaternization reaction in DMF solution. Typically 0.2 g of CIF2 and 0.2 g of dibromoethane (C<sub>2</sub>H<sub>4</sub>Br<sub>2</sub>) in 20 ml DMF was heated and stirred at 80°C for 3 days. After the mixture was cooled to room temperature, obtained black precipitation was immersed into methanol for 12 hours. Afterwards the precipitate was washed thoroughly with methanol and dried at 80°C for 12 hours under vacuum. The yield of CIF2-C<sub>2</sub>H<sub>4</sub> obtained was 0.23 g, (83.2% yield). CIF1-C<sub>2</sub>H<sub>5</sub>, CIF2-C<sub>2</sub>H<sub>5</sub> were synthesized following the same procedure except the dibromoethane was replaced by bromoethane (C<sub>2</sub>H<sub>5</sub>Br) and with 90.5% and 87.4% yield, respectively.

**Synthesis of Zn-CIF1-C<sub>2</sub>H<sub>5</sub>, Zn-CIF2-C<sub>2</sub>H<sub>5</sub> and Zn-CIF2-C<sub>2</sub>H<sub>4</sub>:** Zn-CIF1-C<sub>2</sub>H<sub>5</sub>, Zn-CIF2-C<sub>2</sub>H<sub>5</sub> and Zn-CIF2-C<sub>2</sub>H<sub>4</sub> were prepared by direct metallation of the ionized CIFs with Zn(OAc)<sub>2</sub>·2H<sub>2</sub>O. For Zn-CIF2-C<sub>2</sub>H<sub>4</sub>, 100 mg of CIF2-C<sub>2</sub>H<sub>4</sub> and 500 mg of Zn(OAc)<sub>2</sub>·2H<sub>2</sub>O were added to 100 mL of dried DMF. The mixture was refluxed at 150°C for 6 h. After 6 h the solution was cooled down to room temperature and the solid content was filtered off. The obtained solid was washed thoroughly with methanol and hot water and dried under vacuum at 80°C overnight to remove absorbed solvents. Co-CIF1-C<sub>2</sub>H<sub>5</sub> was prepared following the same synthetic procedure used for Zn-CIF1-C<sub>2</sub>H<sub>4</sub> except that Zn(OAc)<sub>2</sub>·2H<sub>2</sub>O (500 mg) was replaced by Co(OAc)<sub>2</sub>·2H<sub>2</sub>O (500 mg). A yield of 91.1%, 89.6%, 95.3% and 94.0% was noted for Zn-CIF1-C<sub>2</sub>H<sub>5</sub>, Co-CIF1-C<sub>2</sub>H<sub>5</sub>, Zn-CIF2-C<sub>2</sub>H<sub>5</sub> and Zn-CIF2-C<sub>2</sub>H<sub>4</sub>, respectively.

**General procedure for the coupling reactions of CO<sub>2</sub> and epoxides:** The reactions were carried out in a 50 mL stainless steel autoclave equipped with a magnetic stirrer. In a typical experiment, 0.174 mg of PO (3 mmol) and catalysts (0.18 mol. % of PO) were inserted into the reactor at room temperature. After purging the reactor with CO<sub>2</sub> to remove air, the autoclave was pressurized to 2.5 MPa (with CO<sub>2</sub>) and heated for 4–8 hours to 120°C under stirring at 460 rpm. At the end of the reaction, the reactor was quenched in a bath containing a water-ice slurry. When the reaction had cooled, the CO<sub>2</sub> pressure was released from the autoclave. The organic solvent contain liquid products were analyzed by gas chromatograph using a Agilent 7890 GC equipped with a HP-5 column (30 m × 0.25 mm × 0.25 mm). Ethyl acetate was added to serve as the external standard. In the cyclic experiment, the solid catalyst was recovered by centrifugation. The recovered catalyst was washed carefully with methanol and dried under vacuum at 60°C for 3 h before the next cycle.

**Acknowledgements**

This work was financially supported by the National Natural Science Foundation of China (No.21676278, No.21878303), the

## FULL PAPER

Instrument Developing Project of the Chinese Academy of Sciences (No. YZ201624) and The National Key Research and Development Program of China (No.2016YFB0601303). the State Key Laboratory of Organic-Inorganic Composites (No. oic-201503005), and Beijing Natural Science Foundation (2192039).

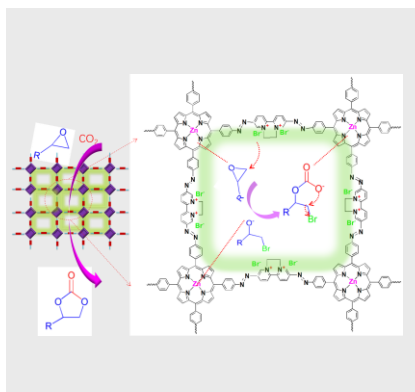
**Keywords:** cooperative catalysis • carbon dioxide • cycloaddition • ionic framework • metalloporphyrin

- [1] a) X. Bao, *Natl. Sci. Rev.* **2015**, *2*, 137-137; b) P. Lanzafame, S. Perathoner, G. Centi, S. Gross, E. J. M. Hensen, *Catal.Sci.Technol.* **2017**, *7*, 5182-5194.
- [2] a) W. Günter, *Chem. Rev.* **2002**, *102*, 1-27; b) N. Straeter, W. N. Lipscomb, T. Klabunde, B. Krebs, *Angew. Chem.* **1996**, *18*, 2159-2191; c) D. Urbano, B. Daniel, C. Avelino, *Chem. Soc. Rev.* **2013**, *42*, 4083-4097.
- [3] a) S. Liu, A. Motta, A. R. Mouat, D. Massimiliano, T. J. Marks, *J. Am. Chem. Soc.* **2014**, *136*, 10460-10469; b) Q. Sun, B. Aguila, J. Perman, N. Nguyen, S. Ma, *J. Am. Chem. Soc.* **2016**, *138*, 15790-15796.
- [4] a) J. An, C. M. Shade, D. A. Chengelis-Czegana, P. Stéphane, N. L. Rosi, *J. Am. Chem. Soc.* **2011**, *133*, 1220-1223; b) Q. Su, Y. Qi, X. Yao, W. Cheng, L. Dong, S. Chen, S. Zhang, *Green Chem.* **2018**, *20*, 1463-9262.
- [5] H. Chen, H. Tu, C. Hu, Y. Liu, D. Dong, Y. Sun, Y. Dai, S. Wang, H. Qian, Z. Lin, *J. Am. Chem. Soc.* **2018**, *140*, 896-899.
- [6] a) S. Jayakumar, H. Li, J. Chen, Q. Yang, *ACS Appl. Mater. Interfaces* **2018**, *10*, 2546-2555; b) D. Ma, K. Liu, J. Li, Z. Shi, *Acs Sustain. Chem. Eng.* **2018**, *6*, 15050-15055.
- [7] S. Cao, B. Li, R. Zhu, H. Pang, *Chem. Eur. J.* **2019**, *355*, 602-623.
- [8] a) K. Dong, X. Liu, H. Dong, X. Zhang, S. Zhang, *Chem. Rev.* **2017**, *117*, 6636-6695; b) S. Zhang, J. Sun, X. Zhang, J. Xin, Q. Miao, J. Wang, *Chem. Soc. Rev.* **2014**, *43*, 7838-7869; c) S. Zhang, N. Sun, X. He, X. Lu, X. Zhang, *J. Phys. Chem. Ref. Data* **2006**, *35*, 1475-1517.
- [9] H. Hu, Q. Yan, M. Wang, L. Yu, W. Pan, B. Wang, Y. Gao, *Chin. J. Catal.* **2018**, *39*, 1437-1444.
- [10] a) A. M. Appel, J. E. Bercaw, A. B. Bocarsly, H. Dobbek, D. L. DuBois, M. Dupuis, J. G. Ferry, E. Fujita, R. Hille, P. J. Kenis, C. A. Kerfeld, R. H. Morris, C. H. Peden, A. R. Portis, S. W. Ragsdale, T. B. Rauchfuss, J. N. Reek, L. C. Seefeldt, R. K. Thauer, G. L. Waldrop, *Chem. Rev.* **2013**, *113*, 6621-6658; b) M. Aresta, A. Dibenedetto, A. Angelini, *Chem. Rev.* **2014**, *114*, 1709-1742.
- [11] B. Xu, J. Wang, J. Sun, Y. Huang, J. Zhang, X. Zhang, S. Zhang, *Green Chem.* **2015**, *17*, 108-122.
- [12] S. Jayakumar, H. Li, L. Tao, C. Li, L. Liu, J. Chen, Q. Yang, *Acs Sustain. Chem. Eng.* **2018**, *6*, 9237-9245.
- [13] M. North, R. Pasquale, C. Young, *Green Chem.* **2010**, *12*, 1514-1539.
- [14] a) J. Chen, M. Zhong, L. Tao, L. Liu, S. Jayakumar, C. Li, H. Li, Q. Yang, *Green Chem.* **2018**, *20*, 903-911; b) W. Jiang, J. Yang, Y. Liu, S. Song, J. Ma, *Chemistry* **2016**, *22*, 16991-16997; c) J. Kim, S. Kim, H. Jang, G. Seo, W. Ahn, *Appl. Catal. A Gel.* **2013**, *453*, 175-180; d) Z. Dai, Q. Sun, X. Liu, C. Bian, Q. Wu, S. Pan, L. Wang, X. Meng, F. Deng, F. Xiao, *J. Catal.* **2016**, *338*, 202-209.
- [15] a) Y. Chen, R. Luo, Q. Xu, J. Jiang, X. Zhou, H. Ji, *ChemSusChem* **2017**, *10*, 2534-2541; b) Y. Chen, R. Luo, Q. Xu, J. Jiang, X. Zhou, H. Ji, *Acs Sustain. Chem. Eng.* **2017**, *6*, 1074-1082.
- [16] N. Manoranjan, S. I. Woo, *Rsc Adv.* **2016**, *6*, 2046-2069.
- [17] H. Li, X. Ding, B. Han, *Chemistry* **2016**, *22*, 11863-11868.
- [18] A. Chen, Y. Zhang, J. Chen, L. Chen, Y. Yu, *J. Mater. Chem. A* **2015**, *3*, 9807-9816.
- [19] J. Liang, Y. Xie, Q. Wu, X. Wang, T. Liu, H. Li, Y. Huang, R. Cao, *Inorg. Chem.* **2018**, *57*, 2584-2593.
- [20] Y. Xu, Z. Li, F. Zhang, X. Zhuang, Z. Zeng, J. Wei, *RSC Adv.* **2016**, *6*, 30048-30055.
- [21] S. Wang, K. Song, C. Zhang, S. Yu, L. Tao, B. Tan, *J. Mater. Chem. A* **2017**, *5*, 1509-1515.
- [22] T. Ema, Y. Miyazaki, J. Shimonishi, C. Maeda, J. Y. Hasegawa, *J. Am. Chem. Soc.* **2016**, *136*, 15270-15279.
- [23] M. Chihoro, T. Tomoya, O. Kanae, E. Tadashi, *Angew. Chem.* **2015**, *46*, 134-138.

## FULL PAPER

## FULL PAPER

We designed new “biomimetic heterogeneous catalyst” : multifunctional metalloporphyrin CIFs with a highly porous structure for cooperative catalysis, which showed efficient catalytic activity in CO<sub>2</sub> cycloaddition and the catalytic performance could be further enhanced by altering the functional groups and the BET surface area.



Jiahui Liu, Guoying Zhao, Ocean Cheung, Lina Jia, Zhenyu Sun\* and Suojiang Zhang\*

Page No. – Page No.

**Highly Porous Metalloporphyrin Covalent Ionic Frameworks with Well Defined Cooperative Functional Groups as Excellent Catalysts for CO<sub>2</sub> Cycloaddition**

Accepted Manuscript